

## Symmetry-resolved C and O *K*-shell photoabsorption spectra of free CO molecules

E. Shigemasa, T. Hayaishi,\* T. Sasaki, and A. Yagishita

*Photon Factory, National Laboratory for High Energy Physics, Oho 1-1, Tsukuba-shi, Ibaraki-ken 305, Japan*

(Received 18 September 1992)

Symmetry-resolved photoabsorption spectra measured at the C and O *K* edges of CO have demonstrated the symmetry decomposition of the conventional photoabsorption spectra. These spectra have been compared with theoretical calculations in the *K*-shell ionization continua. Definite assignments for the symmetries have been given in the photon-energy regions below and above the *K*-shell ionization thresholds.

PACS number(s): 33.80.Eh, 33.80.Gj

### I. INTRODUCTION

The inner-shell photoabsorption spectroscopy of molecules, which is one of the most fundamental probes of their electronic and geometric structures, has a long history of elucidating inner-shell phenomena [1]. However, in spite of intense effort over the past 20 years [1,2], the inner-shell spectra of molecules have not been thoroughly investigated. This has been due to the lack of intense excitation sources. Undulator-radiation sources in the soft-x-ray range now provide tunable, intense, and highly polarized exciting radiation throughout the spectral range of *K*-shell ionization in molecules containing first-row elements. Synchrotron radiation from bending magnets also provides polarized radiation. Although this makes it possible to determine the molecular symmetries of the *K*-shell excited states of small molecules [3–7], the undulator radiation has a great advantage on the degree of linear polarization and on the intensity. Combination of the advantages offered by the undulator radiation with angle-resolved fragment-photoion measurements has enabled us to decompose the photoabsorption spectra into their molecular symmetry components. As a result, it has become possible to determine directly the molecular symmetries of *K*-shell excited states, and to decompose degenerate states in the continuum for diatomic molecules [8–14].

In electric-dipole transitions induced by the linearly polarized light, the transition probabilities relate to the molecular orientation with respect to the direction of the electric vector of the incident light. There are two types of dipole-allowed transitions for the *K*-shell excitations of the diatomic molecules:  $\sigma \rightarrow \sigma$  and  $\sigma \rightarrow \pi$  transitions. Depending on its energy, a monoenergetic soft x ray promotes a *K*-shell electron to an unoccupied valence and Rydberg orbital with a definite symmetry of  $\sigma$  or  $\pi$ , or into the continuum where the  $\sigma$  and  $\pi$  states are degenerate. For the  $\sigma \rightarrow \sigma$  transitions the molecules oriented parallel to the polarization direction are selectively excited, while for the  $\sigma \rightarrow \pi$  transitions the molecules oriented perpendicular to the direction are preferentially excited from a random ensemble of free molecules [15–17]. The molecular orientation will be directly reflected in the angular distribution of fragment photoions emitted immedi-

ately from a repulsive potential of molecular ions, which is reached by a fast Auger decay of the *K*-shell vacancy ( $\tau \sim 10^{-14}$  sec) compared to molecular rotation periods ( $\tau \sim 10^{-10}$  sec).

In previous papers, we have reported the symmetry-resolved *K*-shell absorption spectra of N<sub>2</sub>, O<sub>2</sub>, and NO molecules [11–14], demonstrating the symmetry decomposition of the conventional absorption spectra. In this paper, we present the symmetry-resolved C and O *K*-shell absorption spectra of CO molecules. Although the measurements on the Auger emission anisotropy of CO were done by Truesdale *et al.* [18] and Becker *et al.* [19], the two groups could not indicate clear information on the molecular orientation after *K*-shell photoexcitation except for the first  $\pi^*$  resonance. The angle-resolved fragment-photoion measurement technique reported here provides a significant new approach to molecular photoabsorption: a direct method for determining the symmetries by the decomposition of the absorption spectra. The dynamics of the photoionization process, i.e., the spectral intensities of individual symmetries as a function of photon energy, will be discussed comparing our symmetry-resolved absorption spectra with available theoretical results.

### II. EXPERIMENT

Here we mention the experimental setup and procedure briefly, since they have been described in detail elsewhere [11]. The experiments have been performed on beam line BL-2B supplying the synchrotron radiation emitted from an undulator [20] inserted in the 2.5-GeV storage ring at the Photon Factory. The radiation was monochromatized by a 10-m grazing-incidence monochromator [21] equipped with an Au-coated replica grating of 1200 grooves/mm. Two identical parallel-plate electrostatic energy analyzers with position-sensitive detectors [22] were used to measure fragment photoions. The analyzers were positioned to detect the photoions emitted at 0° and 90° with respect to the electric vector of the incident light, respectively. The  $\Sigma$  symmetry component spectrum ( $\sigma_{\Sigma}$ ) was obtained by counting the signals for the energetic fragment ions ( $\geq 2$  eV), detected by the 0° positioned analyzer, as a function of the photon en-

ergy. The  $\Pi$  symmetry component ( $\sigma_{\Pi}/2$ ) was obtained by the same procedure using the  $90^\circ$  positioned analyzer. The two spectra were measured simultaneously by the single scan of the monochromator. The photon-energy scale was calibrated on the basis of the electron energy-loss spectra reported by Hitchcock and Brion [23].

The different detection efficiencies of the two analyzers have been corrected using the same coefficient as determined in the experiment for  $N_2$  [11], because the experimental arrangement has been unchanged during the course of the measurements. The valence contributions are considered as being constant in the  $K$ -shell excitation regions. We have subtracted the constant valence contributions from the  $\sigma_{\Sigma}$  and  $\sigma_{\Pi}/2$  spectra. In the O  $K$ -shell excitation region, the spectra are composed of the C and O  $K$ -shell contributions. We have assumed the C  $K$ -shell contribution has been monotonically decreasing in the O  $K$ -shell excitation region, and subtracted it from the O  $K$ -shell excitation spectra. In order to obtain  $\sigma_{\Pi}$ , the  $\sigma_{\Pi}/2$  spectrum has been multiplied by a factor of 2 after the background subtractions. These procedures have been done for the spectra displayed in the following sections.

### III. RESULTS AND DISCUSSIONS

#### A. C $K$ -shell excitation of CO

##### 1. Overview

Figure 1(a) shows the  $\sigma_{\Sigma}$  and  $\sigma_{\Pi}$  symmetry-resolved C  $K$ -edge photoabsorption spectra of CO, which have been measured with a monochromator bandpass of 0.29 eV. The dots and the solid line represent  $\sigma_{\Sigma}$  and  $\sigma_{\Pi}$ , respectively. One can construct a conventional photoabsorption spectrum shown in Fig. 1(b) by adding  $\sigma_{\Sigma}$  to  $\sigma_{\Pi}$ . Although the sum spectrum in Fig. 1(b) is comparable with the photoabsorption spectrum, there are some differences regarding the intensities between them. We have measured only the energetic fragment ions ( $\geq 2$  eV) to obtain the  $\sigma_{\Sigma}$  and  $\sigma_{\Pi}$  symmetry-resolved spectra. However, resonance Auger decays can lead to singly charged molecular ions mainly, and produce nonenergetic fragment ions or undissociated molecular ions. Therefore the signal intensities of our spectrum may be weaker than those of the photoabsorption spectrum below the ionization threshold.

The spectral features ( $A-F$ ) of the sum spectrum in Fig. 1(b) closely resemble the electron energy-loss spectra [23–25]. The sum spectrum is dominated by a very intense peak  $A$  due to the transition of a C  $1s$  electron into an unoccupied  $2p\pi^*$  valence orbital. Above the  $1s \rightarrow 2p\pi^*$  transition, the spectrum exhibits weak structures ( $B-D$ ) up to the ionization limit. These are assigned to the promotions of the C  $1s$  electron into Rydberg states. In the continuum two broad bands of  $E$  and  $F$  appear. The band  $E$  is attributable to double excitations, and  $F$  is assigned to a  $\sigma^*$  continuum shape resonance.

Only the excited states with  $\Sigma$  symmetry should be observed in the symmetry-resolved  $\sigma_{\Sigma}$  spectrum. The  $\sigma_{\Sigma}$

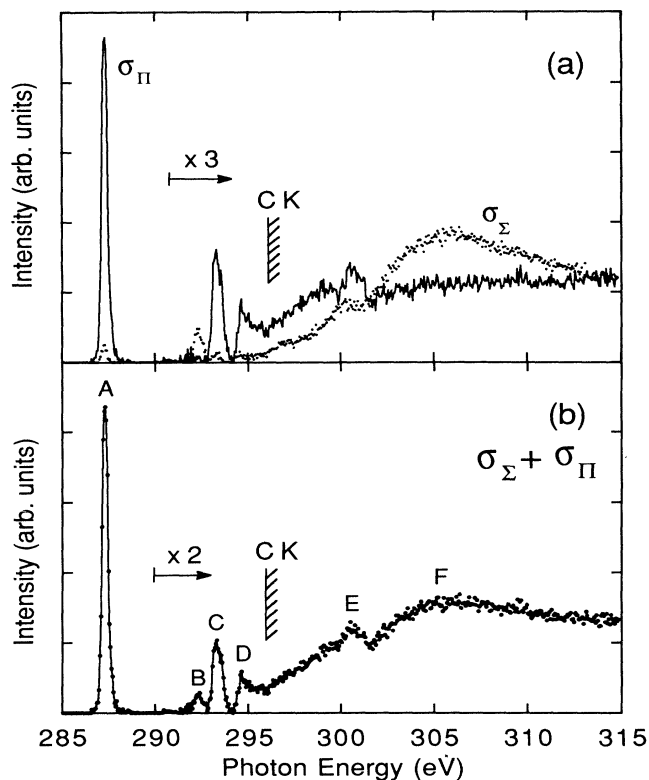


FIG. 1. (a)  $\sigma_{\Sigma}$  (dots) and  $\sigma_{\Pi}$  (solid line) symmetry-resolved C  $K$ -edge photoabsorption spectra of CO. (b) Sum of the  $\sigma_{\Sigma}$  and  $\sigma_{\Pi}$  symmetry-resolved C  $1s$  photoabsorption spectra of CO. The spectra in (a) and (b) have been multiplied by a factor of 3 and 2 in the photon-energy regions above the horizontal bars, respectively.

spectrum is mainly composed of the broad peak  $F$  due to the  $\sigma^*$  shape resonance, and the weak peak  $B$  corresponding to a Rydberg state with  $\Sigma$  symmetry [Fig. 1(a)]. On the other hand, only the excited states with  $\Pi$  symmetry are observed in the symmetry-resolved  $\sigma_{\Pi}$  spectrum. The  $\sigma_{\Pi}$  spectrum is comprised of the very intense peak  $A$  for the excitation to a  $2p\pi^*$  state, the weak peaks of  $C$  and  $D$  for Rydberg states, and the rather strong structure  $E$  corresponding to doubly excited states [Fig. 1(a)]. The weak peak in  $\sigma_{\Sigma}$  at the  $2p\pi^*$  resonance energy of 287.3 eV may be caused by the insufficient degree of the linear polarization of the incident light, because one cannot expect to detect any signals in  $\sigma_{\Sigma}$  for a pure  $\sigma \rightarrow \pi$  transition like the  $2p\pi^*$  excitation. The degree of the linear polarization at 287.3 eV was estimated to be 90% by the same procedure that was described in the Ref. [11].

##### 2. Discrete resonances

Figure 2 shows the blowup of the  $\sigma_{\Sigma}$  and  $\sigma_{\Pi}$  symmetry-resolved photoabsorption spectra below the C  $K$ -shell ionization threshold of CO. In the  $\sigma_{\Pi}$  spectrum, a very intense peak  $A$  and a weak peak  $C$  are found. The peak  $A$  is attributed to the excitation of the C  $1s$  electron into an unoccupied  $2p\pi^*$  valence orbital as mentioned in

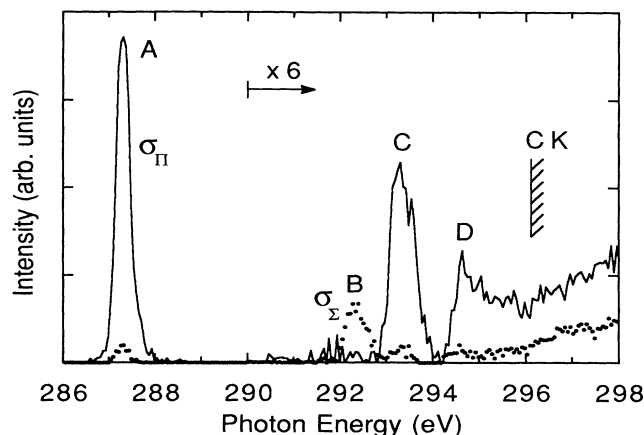


FIG. 2. Blowup of  $\sigma_{\Sigma}$  (dots) and  $\sigma_{\Pi}$  (solid line) spectra below the ionization limit. The spectra have been multiplied by a factor of 6 in the photon-energy region above the horizontal bar.

Sec. III A 1. The peak *C* corresponds to a promotion of the  $1s$  electron into the  $3p\pi$  Rydberg orbital. In the  $\sigma_{\Sigma}$  spectrum, the weak peak *B* corresponding to the transition of the  $1s$  electron into the  $3s\sigma$  Rydberg orbital is observed.

Beneath the peak *C* in the  $\sigma_{\Pi}$  spectrum, a very weak peak for the  $3p\sigma$  Rydberg orbital excitation can be seen in  $\sigma_{\Sigma}$ . This peak has not been resolved yet despite the great efforts of high-resolution work [26–28], because the two states have different symmetries but almost the same excitation energies. However, the present method has enabled us to resolve the peak *C* in Fig. 1(b) into the two peaks having different symmetries. The peak intensity ratio of the  $3p\sigma$  state to the  $3p\pi$  state is  $\sim 0.09$ . Assuming that the degree of linear polarization is 90%, the intensi-

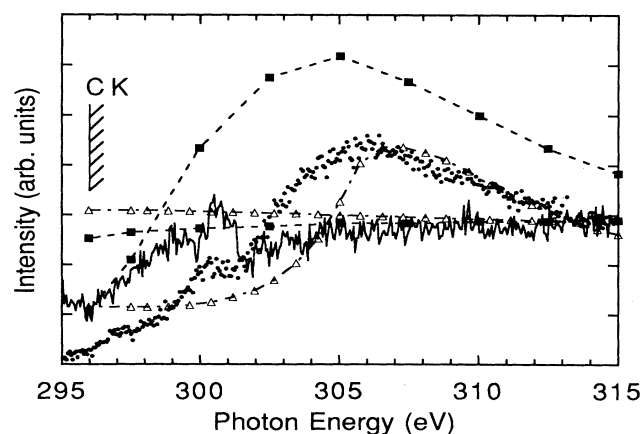


FIG. 3. Blowup of  $\sigma_{\Sigma}$  (dots) and  $\sigma_{\Pi}$  (solid line) spectra in the *C K*-shell ionization continuum region of CO, together with *ab initio* calculations. The dashed curves with filled squares represent the results of the STMT calculations by Padiál *et al.* [30]. The dot-dashed curves with open triangles denote the results of the RCHF calculations by Schirmer, Braunstein, and McKoy [31].

ty ratio becomes  $\sim 0.04$ . This is in good agreement with the theoretically predicted value of  $\sim 0.04$  by Barth and Schirmer [29].

Between 294.2 and 296.0 eV, there are unresolved Rydberg structures *D* in both  $\sigma_{\Sigma}$  and  $\sigma_{\Pi}$ . These Rydberg states have been resolved and assigned by Tronc, King, and Read [26], Domke *et al.* [27], and Ma *et al.* [28]. These authors have reached the same assignments for the observed Rydberg states on the basis of the equivalent-core model; the structures between 294.2 and 296.0 eV are composed of the main  $np\pi$  ( $n \geq 4$ ) and rather weak  $nd\pi$  ( $n \geq 3$ ) Rydberg series. The  $4p\pi$  Rydberg excitation is about twice the strength of the  $3d\pi$  excitation. In our high-resolution work, we have also observed the Rydberg series and confirmed these assignments [14]. Although the fine structures of the Rydberg series can hardly be seen in Fig. 2, the  $\Pi$  component is predominant between 294.2 and 296.0 eV. From our symmetry-resolved spectra, it has become clear that the photoabsorption in this region is comprised of the main  $np\pi$  ( $n \geq 4$ ) and  $nd\pi$  ( $n \geq 3$ ) Rydberg series and extremely minor  $ns\sigma$  ( $n \geq 4$ ) and  $np\sigma$  ( $n \geq 4$ ) series.

### 3. Double excitations and continuum

Figure 3 shows the blowup of the symmetry-resolved  $\sigma_{\Sigma}$  and  $\sigma_{\Pi}$  photoabsorption spectra together with *ab initio* calculations in the continuum region. The dashed curves with filled squares represent the results of Stieltjes-Tchebycheff moment-theory (STMT) calculations by Padiál *et al.* [30], and the dot-dashed curves with open triangles represent the results of relaxed-core Hartree-Fock (RCHF) calculations by Schirmer, Braunstein, and McKoy [31]. The  $\Pi$  component of these calculations have been normalized to the experimental  $\sigma_{\Pi}$  at 315 eV. Double excitations observed around 300 eV are not taken into account in these calculations.

According to the theoretical calculations by Ågren and Arneberg [32], the possible doubly-excited states are interpreted as  $2p\pi \rightarrow 3p\pi$ ,  $2p\sigma \rightarrow 3p\sigma$ , and  $2s\sigma \rightarrow 2p\pi^*$  shake-up transitions in the course of the  $C 1s \rightarrow 2p\pi^*$  excitation. The former two have  $\Pi$  symmetry, and the latter one has  $\Sigma$  symmetry. The transition energies and relative intensities for these shake-up states are given in their paper: 305.31 eV, 4.15 ( $2p\pi^{-1}2p\pi^*3p\pi$ ), 307.25 eV, 3.58 ( $2p\sigma^{-1}2p\pi^*3p\sigma$ ), and 304.05 eV, 3.11 ( $2s\sigma^{-1}2p\pi^*2p\pi^*$ ). Kosugi has also made theoretical calculations for the doubly-excited states and reported that the main configuration of these states has a  $\Pi$  component [33]. The calculated transition energy is 303.2 eV. In our  $\sigma_{\Pi}$  spectrum, the broad structure due to the double excitations are observed around 299 and 300.6 eV. The weak bump is seen at 300.2 eV in the  $\sigma_{\Sigma}$  spectrum. Although differences between the experiment and calculation are left, the theoretical results of Ågren and Arneberg [32] suggesting three groups of the shake-up transitions are consistent with the experiment.

The  $\sigma^*$  shape resonance is observed as the very broad enhancement of the photoabsorption in the  $\sigma_{\Sigma}$  spectrum. The  $\sigma_{\Sigma}$  contribution is almost equal to the  $\sigma_{\Pi}$  even at 20 eV above the threshold, differing from the statistical ratio

of 1:2. It means that the  $\sigma^*$  shape resonance effect spreads over an extremely wide energy range. For the STMT calculations, the  $\sigma^*$  shape resonance is overestimated over the whole energy region. On the other hand, the RCHF calculations taking the core-relaxation effect into account give better quantitative agreement with the experimental results, except for the discrepancy below 305 eV.

The main reason the STMT calculations give unsatisfactory results may be attributable to the effects of the core relaxation, as discussed by Schirmer, Braunstein, and McKoy [31] and Lynch and McKoy [34]. The STMT calculations have been carried out in the frozen-core Hartree-Fock (FCHF) approximation which excludes relaxation effects. The FCHF potential is too attractive due to the neglect of screening of the  $K$ -shell hole by the valence electrons. As a result, the use of the FCHF approximation leads to the underestimation of the  $\sigma^*$  resonance energy and the overestimation of its intensity.

The overall  $\sigma_{\Pi}$  spectrum including the double excitations is quite similar to the case of the  $K$ -shell ionization of  $N_2$  in Ref. [11]. Neglecting the contribution of the double excitations around 300 eV, the  $\sigma_{\Pi}$  spectrum increases monotonically up to 304 eV and becomes almost constant above 304 eV. The STMT results for the  $\Pi$  symmetry component give a monotonically increasing behavior, while the RCHF calculations give a monotonically decreasing cross section in the energy region shown in Fig. 3. However, the suppression of the  $C\ 1s\sigma \rightarrow \varepsilon\pi$  transitions in the ionization-threshold region, which was revealed by our symmetry-resolved absorption spectrum, is not explained by present available theoretical calculation.

## B. O $K$ -shell excitation

### 1. Overview

Figure 4(a) shows the  $\sigma_{\Sigma}$  and  $\sigma_{\Pi}$  symmetry-resolved photoabsorption spectra of the O  $K$ -edge of CO with the monochromator bandpass of 0.45 eV. The dots and the solid line represent  $\sigma_{\Sigma}$  and  $\sigma_{\Pi}$ , respectively. The sum of the  $\sigma_{\Sigma}$  and  $\sigma_{\Pi}$  spectra of CO is shown in Fig. 4(b), which is comparable with the conventional photoabsorption spectrum. The spectral features ( $A-E$ ) of the sum spectrum have already been observed in the electron energy-loss spectra [23,24]. The overall profile of the sum spectrum is very similar to the electron energy-loss spectra. Below the O  $K$ -shell ionization threshold, the sum spectrum is dominated by a very intense peak  $A$  due to the O  $1s \rightarrow 2p\pi^*$  transition. Above the  $2p\pi^*$  resonance the spectrum shows very weak structures ( $B-D$ ) up to the threshold, which are assigned to the Rydberg transitions with definite symmetries. In the continuum, only one broad band of  $E$  is observed in contrast to the case of the C  $1s$  ionization. Hitchcock and Brion have considered the band  $E$  as a  $\sigma^*$  continuum shape resonance enhancement [23].

The  $\sigma_{\Sigma}$  spectrum of Fig. 4(a) comprises a broad enhancement due to the  $\sigma^*$  shape resonance, and weak structures for the excitations to the Rydberg states with

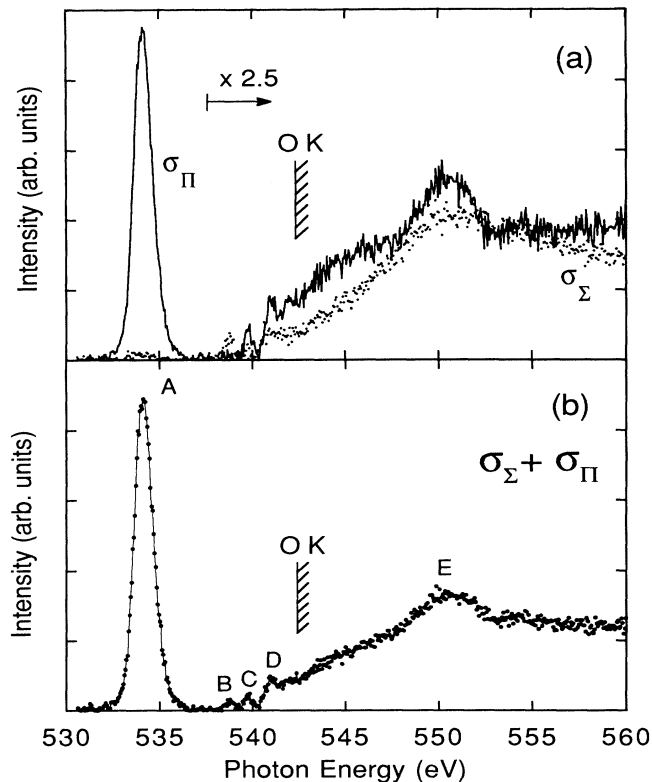


FIG. 4. (a)  $\sigma_{\Sigma}$  (dots) and  $\sigma_{\Pi}$  (solid line) symmetry-resolved O  $K$ -edge photoabsorption spectra of CO. The spectra have been multiplied by a factor of 2.5 in the photon-energy region above the horizontal bar. (b) Sum of the  $\sigma_{\Sigma}$  and  $\sigma_{\Pi}$  symmetry-resolved O  $1s$  photoabsorption spectra of CO.

$\Sigma$  symmetry. The  $\sigma_{\Pi}$  spectrum is composed of a strong peak corresponding to the excitation to the  $2p\pi^*$  valence orbital, weak peaks for Rydberg states, and a strong bump in the continuum which may be due to the double excitations.

### 2. Discrete resonances

The blowup of the  $\sigma_{\Sigma}$  and  $\sigma_{\Pi}$  symmetry-resolved photoabsorption spectra below the O  $K$ -shell ionization threshold of CO are shown in Fig. 5. In the  $\sigma_{\Pi}$  spectrum, a very intense peak  $A$  and weak peaks  $C$  and  $D$  are seen. The peak  $A$  is attributed to the excitation of the O  $1s$  electron into the unoccupied  $2p\pi^*$  valence molecular orbital. The peak  $C$  can be attributed to the O  $1s \rightarrow 3p\pi$  Rydberg transition. The peak  $D$  is due to the unresolved Rydberg series. Compared with the C  $1s$  excitation, it can be seen that the relative intensity of the peak  $C$  to the peak  $D$  is fairly weaker than that in Fig. 2. This implies that the  $3d\pi$  Rydberg transition is much stronger than the  $4p\pi$  Rydberg transition in the O  $K$  edge, in contrast to the case of the C  $K$  edge, which is also supported by the configuration-interaction (CI) calculation of Kosugi [35]. In the  $\sigma_{\Sigma}$  spectrum, the weak peak  $B$  corresponding to the O  $1s \rightarrow 3s\sigma$  transition is seen. Beneath the peak  $C$  in the  $\sigma_{\Pi}$  spectrum, a very weak peak can be seen in  $\sigma_{\Sigma}$ ,

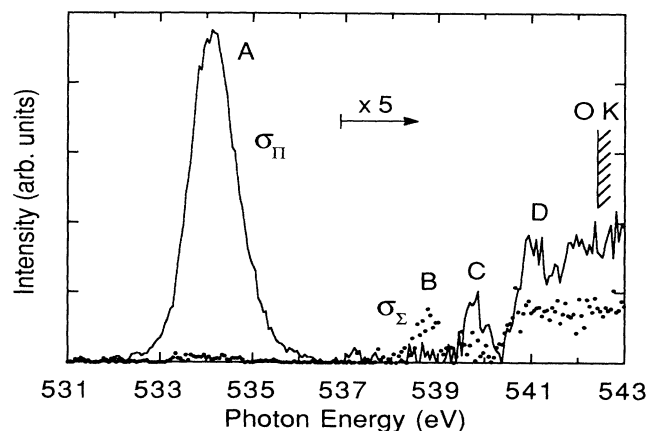


FIG. 5. Blowup of  $\sigma_{\Sigma}$  (dots) and  $\sigma_{\Pi}$  (solid line) spectra below the ionization limit. The spectra have been multiplied by a factor of 5 in the photon-energy region above the horizontal bar.

which can be attributed to the O  $1s \rightarrow 3p\sigma$  transition as in the case of the C  $1s$  excitation. The peak intensity ratio of the  $3p\sigma$  state to the  $3p\pi$  state is about 0.5.

Between 540.2 and 542.4 eV, there are some structures which correspond to the excitation to Rydberg states. The fine structures of these Rydberg states have been resolved and assigned by Domke *et al.* [27]. The authors have given the assignments for the observed Rydberg states on the basis of the equivalent core model; the structures between 540.2 and 542.4 eV are composed of the main  $np\pi$  ( $n \geq 4$ ) and rather weak  $nd\pi$  ( $n \geq 3$ ) Rydberg series. However, the intensity ratio of the peak C to the peak D in Fig. 5 and the results of the CI calculations by Kosugi [35] strongly suggest that the  $nd\pi$  ( $n \geq 3$ ) Rydberg series are stronger than the  $np\pi$  ( $n \geq 4$ ) series. Although it is very hard to see the fine structures of the higher Rydberg series in Fig. 5, the series between 540.2 and 542.4 eV are obviously dominated by the  $\Pi$  component, but there are considerable contributions of the  $\Sigma$  component in contrast to the case of the C  $K$  edge.

### 3. Double excitations and continuum

The  $\sigma_{\Sigma}$  and  $\sigma_{\Pi}$  symmetry-resolved photoabsorption spectra above the O  $K$ -shell ionization threshold are shown in Fig. 6, together with *ab initio* calculations. The dashed curves with filled squares represent the results of the STMT calculations of Padiál *et al.* [30]. The dot-dashed curves with open triangles represent the results of the RCHF calculations of Schirmer, Braunstein, and McKoy [31]. The  $\Pi$  component of each calculation has been normalized to the experimental  $\sigma_{\Pi}$  at 560 eV. Double excitations observed around 551 eV are not taken into account in these calculations.

Although the possibilities for the double excitation were proposed theoretically by Ågren and Arneberg [32], the doubly-excited states in the O  $1s$  continuum have not been noticed yet experimentally, because the conventional photoabsorption spectra give only one broadband similar to the  $\sigma^*$  shape resonance enhancement in the continuum [see Fig. 4(b)]. However, the doubly-excited states

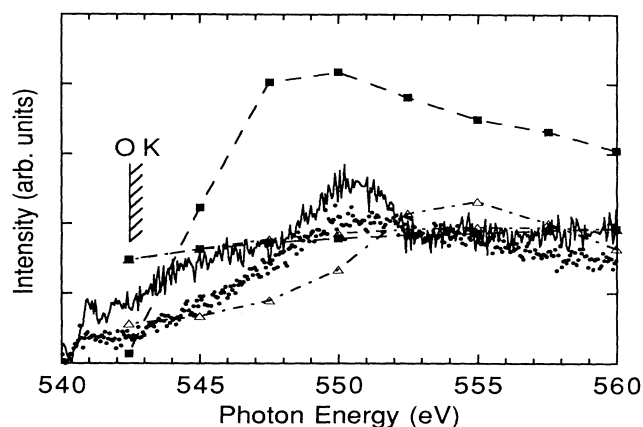


FIG. 6. Blowup of  $\sigma_{\Sigma}$  (dots) and  $\sigma_{\Pi}$  (solid line) spectra in the O  $K$ -shell ionization continuum region of CO, together with *ab initio* calculations. The dashed curves with filled squares represent the results of the STMT calculations by Padiál *et al.* [30]. The dot-dashed curves with open triangles denote the results of the RCHF calculations by Schirmer, Braunstein, and McKoy [31].

with  $\Pi$  symmetries are revealed in the  $\sigma_{\Pi}$  spectrum, separated from the  $\sigma^*$  shape resonance seen in the  $\sigma_{\Sigma}$  spectrum, by the present symmetry-resolved measurements.

According to the CI calculations by Ågren and Arneberg [32], the main configuration of the doubly excited states can be attributed to the O  $1s \rightarrow 2p\pi^*$  transition with a  $2p\pi \rightarrow 2p\pi^*$  shake-up. The calculated excitation energy of this state is about 555 eV, which is 4 eV higher than the experimental peak position of 551 eV. The present result for the double excitations supports the symmetry assignment by Ågren and Arneberg [32], that is, the total symmetry of the dominant configuration of the doubly-excited states is  $\Pi$ .

The intensity of the  $\Sigma$  component including the  $\sigma^*$  shape-resonance enhancement is comparable with that of the  $\Pi$  component excluding the double-excitation contribution over the whole energy range in Fig. 6. In contrast to this symmetry-resolved experimental result, the STMT calculations give the intensity for  $\sigma_{\Sigma}$  being about twice the strength of that for  $\sigma_{\Pi}$ . This serious discrepancy was not encountered in the comparison of the theoretical results with the conventional photoabsorption spectra. On the other hand, the RCHF calculations agree pretty well with the present  $\sigma_{\Sigma}$  and  $\sigma_{\Pi}$  spectra except for the peak position of the  $\sigma^*$  shape resonance. As observed above the C  $K$  edge, the  $\sigma^*$  resonance does enhance the intensity of the  $\Sigma$  component only. This enhancement relative to the intensity of the  $\Pi$  component above the O  $K$  edge is less pronounced than that above the C  $K$  edge. Such a site-specific behavior of the  $\sigma^*$  resonance has already been predicted by the continuum state multiple-scattering calculations by Dill *et al.* [17], although their results overestimate the resonance effect. The more sophisticated RCHF calculations now show good agreement with the present results in both cases, the C  $1s$  and O  $1s$  ionization.

## IV. SUMMARY

From our symmetry-resolved C and O *K*-edge absorption spectra, definite assignments for the symmetries of the *K*-shell excited states have been given in the photon-energy regions below and above the ionization thresholds. For the Rydberg excitations of both C and O *K* edges, the overlapping of the weak  $3p\sigma$  Rydberg state and the  $3p\pi$  state has been resolved. It has also become clear that the higher Rydberg series have been mainly composed of the  $\Pi$  symmetry components. The present  $\sigma_{\Sigma}$  and  $\sigma_{\Pi}$  spectra have resolved the doubly-excited states from the  $\sigma^*$  shape resonance enhancements in the C and O *K*-shell ionization continua. Especially for the O *K*-shell ionization continuum, the present method has enabled us to reveal the doubly-excited states experimentally. The

theoretical calculations by Schirmer, Braunstein, and McKoy [31] give quantitative agreement with the present  $\sigma_{\Sigma}$  and  $\sigma_{\Pi}$  spectra in the  $\sigma^*$  shape resonance regions, except for the resonance positions. For the double excitations, the present results support the symmetry assignments by Ågren and Arneberg [32] and Kosugi [33] at the C *K* edge, and those by Ågren and Arneberg [32] at the O *K* edge.

## ACKNOWLEDGMENTS

We are grateful to the staff of the Photon Factory for the stable operation of the storage ring during the course of the experiments. This work has been performed under approval of the Photon Factory Advisory Committee (Proposal No. 88-185, 90-237).

\*Permanent address: Institute of Applied Physics, University of Tsukuba, Tennodai 1-1, Tsukuba-shi, Ibaraki-ken 305, Japan.

- [1] A. P. Hitchcock, *J. Electron Spectrosc. Relat. Phenom.* **25**, 245 (1982) (a bibliography of inner-shell excitation studies).
- [2] For example, *EXAFS and Near Edge Structure*, edited by A. Bianconi, L. Incoccia, and S. Stipcich, Springer Series in Chemical Physics Vol. 27 (Springer-Verlag, New York, 1983); I. Nenner, in *Electron and Atomic Collisions*, edited by H. B. Gilbody, W. R. Newell, F. H. Read, and A. C. H. Smith (North-Holland, Amsterdam, 1988), p. 517, and references therein.
- [3] D. Lindle, P. L. Cowan, R. E. LaVilla, T. Jach, R. D. Deslattes, B. Karlin, J. A. Sheehy, T. J. Gil, and P. W. Langhoff, *Phys. Rev. Lett.* **60**, 1010 (1988).
- [4] N. Saito and I. H. Suzuki, *Phys. Rev. Lett.* **61**, 2740 (1988).
- [5] N. Saito and I. H. Suzuki, *J. Phys. B* **22**, L517 (1989).
- [6] K. Lee, D. Y. Kim, C. I. Ma, D. A. Lapiano-Smith, and D. M. Hanson, *J. Chem. Phys.* **93**, 7936 (1990).
- [7] R. Mayer, D. W. Lindle, S. H. Southworth, and P. L. Cowan, *Phys. Rev. A* **43**, 235 (1991).
- [8] A. Yagishita, H. Maezawa, M. Ukai and E. Shigemasa, *Phys. Rev. Lett.* **62**, 36 (1989).
- [9] E. Shigemasa, K. Ueda, Y. Sato, T. Hayaishi, H. Maezawa, T. Sasaki and A. Yagishita, *Phys. Scr.* **41**, 63 (1990).
- [10] A. Yagishita and E. Shigemasa, *Rev. Sci. Instrum.* **63**, 1383 (1992).
- [11] E. Shigemasa, K. Ueda, Y. Sato, T. Sasaki, and A. Yagishita, *Phys. Rev. A* **45**, 2915 (1992).
- [12] N. Kosugi, E. Shigemasa, and A. Yagishita, *Chem. Phys. Lett.* **190**, 481 (1992).
- [13] N. Kosugi, J. Adachi, E. Shigemasa, and A. Yagishita, *J. Chem. Phys.* (to be published).
- [14] A. Yagishita, E. Shigemasa, J. Adachi, and N. Kosugi, *Proceedings of the 10th International Conference on Vacuum Ultraviolet Radiation Physics* (World Scientific, Singapore, to be published).
- [15] J. L. Dehmer and D. Dill, *Phys. Rev. A* **18**, 164 (1978).
- [16] S. Wallace and D. Dill, *Phys. Rev. B* **17**, 1692 (1978).
- [17] D. Dill, J. R. Swanson, S. Wallace, and J. L. Dehmer, *Phys. Rev. Lett.* **45**, 1393 (1980).
- [18] C. M. Truesdale, S. H. Southworth, P. H. Kobrin, U. Becker, D. W. Lindle, H. G. Kerkhoff, and D. A. Shirley, *Phys. Rev. Lett.* **50**, 1265 (1983).
- [19] U. Becker, R. Holz, H. G. Kerkhoff, B. Langer, D. Szostak, and R. Wehlitz, *Phys. Rev. Lett.* **56**, 1445 (1986).
- [20] H. Maezawa, Y. Suzuki, H. Kitamura, and T. Sasaki, *Appl. Opt.* **25**, 3260 (1986).
- [21] A. Yagishita, S. Masui, A. Toyoshima, H. Maezawa, and E. Shigemasa, *Rev. Sci. Instrum.* **63**, 1351 (1992).
- [22] A. Yagishita, *Jpn. J. Appl. Phys.* **25**, 657 (1986).
- [23] A. P. Hitchcock and C. E. Brion, *J. Electron Spectrosc. Relat. Phenom.* **18**, 1 (1980).
- [24] G. R. Wight, C. E. Brion, and M. J. Van der Wiel, *J. Electron Spectrosc. Relat. Phenom.* **1**, 457 (1972/1973).
- [25] R. B. Kay, Ph. E. van der Leeuw, and M. J. Van der Wiel, *J. Phys. B* **10**, 2513 (1977).
- [26] M. Tronc, G. C. King, and F. H. Read, *J. Phys. B* **12**, 137 (1979).
- [27] M. Domke, C. Xue, A. Puschnann, T. Mandel, E. Hudson, D. A. Shirley, and G. Kaindl, *Chem. Phys. Lett.* **173**, 122 (1990).
- [28] Y. Ma, C. T. Chen, G. Meigs, K. Randall, and F. Sette, *Phys. Rev. A* **44**, 1848 (1991).
- [29] A. Barth and J. Schirmer, *J. Phys. B* **18**, 867 (1985).
- [30] N. Padial, G. Csanak, V. McKoy, and P. W. Langhoff, *J. Chem. Phys.* **69**, 2992 (1978).
- [31] J. Schirmer, M. Braunstein, and V. McKoy, *Phys. Rev. A* **41**, 283 (1990).
- [32] H. Ågren and R. Arneberg, *Phys. Scr.* **30**, 55 (1984).
- [33] N. Kosugi, in *Core-Level Spectroscopy in Condensed Systems*, edited by J. Kanamori and A. Kotani, Springer Series in Solid-State Sciences Vol. 81 (Springer-Verlag, Berlin, 1988), p. 203.
- [34] D. L. Lynch and V. McKoy, *Phys. Rev. A* **30**, 1561 (1984).
- [35] N. Kosugi (private communication).